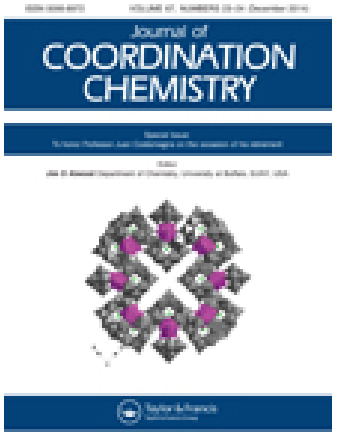

Journal of Coordination Chemistry
Publication details, including instructions for authors and subscription information:
http://www.tandfonline.com/loi/gcoo20

Review: Properties and chemical reactivity of metallo phthalocyanine and tetramethylbenzoannulene complexes grafted into a polymer backbone

G. Ferraudi[a] & A.G. Lappin[a]
[a] Department of Chemistry and Biochemistry, University of Notre Dame, Notre Dame, IN, USA
Accepted author version posted online: 14 Oct 2014.Published online: 10 Nov 2014.

To cite this article: G. Ferraudi & A.G. Lappin (2014) Review: Properties and chemical reactivity of metallo phthalocyanine and tetramethylbenzoannulene complexes grafted into a polymer backbone, Journal of Coordination Chemistry, 67:23-24, 3822-3839, DOI: 10.1080/00958972.2014.975221

To link to this article: http://dx.doi.org/10.1080/00958972.2014.975221

Journal of Coordination Chemistry, 2014
Vol. 67, Nos. 23–24, 3822–3839, http://dx.doi.org/10.1080/00958972.2014.975221

Review: Properties and chemical reactivity of metallo phthalocyanine and tetramethylbenzoannulene complexes grafted into a polymer backbone

G. FERRAUDI* and A.G. LAPPIN

Department of Chemistry and Biochemistry, University of Notre Dame, Notre Dame, IN, USA

(*Received 15 July 2014; accepted 25 September 2014*)

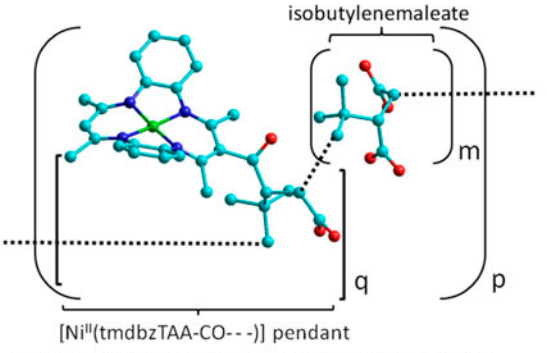

Average structure assigned to the repeating unit of a polymer containing grafted Ni(II) benzoannulene.

The properties of coordination complexes grafted to a polymer backbone are reviewed in this article. The focus is on complexes of phthalocyanine and tetraazaannulene (5,7,12,14-tetramethyldibenzo[b,i][1,4,8,11]tetraazacyclotetradecine, also abbreviated tmdbztaa) with various transition metal ions and Al(III). In addition to the morphological characteristics of the materials, their thermal and photochemical reactions are reviewed. Processes such as catalysis of the lignin degrading process and the reduction of CO_2 are presented as examples of these materials potential applications.

Keywords: Coordination complexes; Polymers; Morphology; Thermal reactions; Photochemistry

Introduction

The extensive and diverse chemistry of transition metal coordination complexes can be modified when the complexes are grafted into a polymer backbone. This extends the chemistry to different conditions that can be used for practical applications [1–9]. There has been

*Corresponding author. Email: ferraudi.1@nd.edu

an increasing interest in the design, synthesis, and use of diverse macrocyclic receptors capable of selective recognition of metal ions, anions, and neutral molecules [10–24]. Such macrocyclic receptors are readily incorporated in polymer matrices. In this role, polyaza-macrocycles have been extensively studied [11–16] because they are able to coordinate divalent metal cations, such as Ni^{2+} or Cu^{2+}, by displacing the amide protons. The complexes have many applications in catalysis [23], molecular machines, oxygen uptake [18, 19], medicine [18], as antiviral agents [25–27], and can also be studied as biological models for metalloproteins [28] in a polymeric environment. For example, the structural features of the macrocycles and the unique radiophysical properties of copper radioisotopes have led to their potential usefulness in diagnostic and/or therapeutic applications [29].

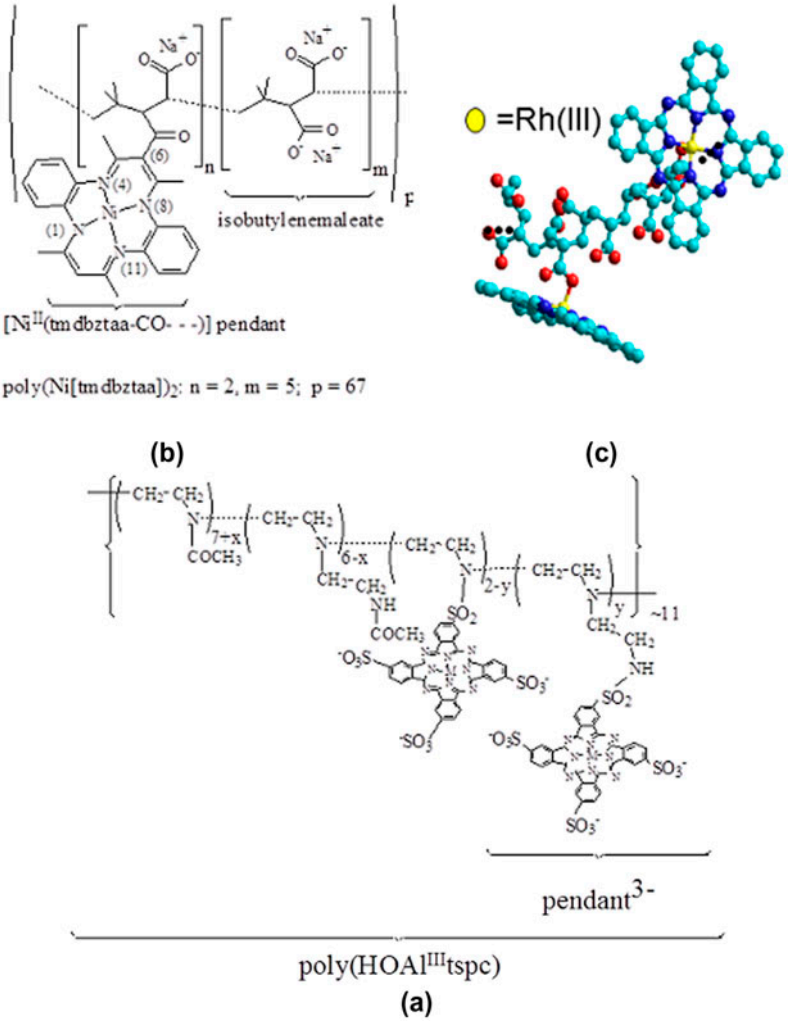

Figure 1. Average formulae of the repeating units assigned to various polymers. The abbreviations of the pendants used in the text are indicated with each formula.

Among the metal complexes that can be grafted into a polymer, the annuleno and phthalocyanine ligands are of a particular interest because they can catalyze thermal and photochemical reactions. In addition to other applications, these complexes are competent in the photoinduced oxidative degradation of lignin [30, 31] and the reduction of CO_2 to CO leading to the photoproduction of strategic materials and the storage of solar energy.

Morphological considerations

To know the morphology of polymers containing grafted coordination complexes is essential for understanding their physical and chemical properties. The different morphologies of polymers either containing grafted coordination complexes or resulting from the polymerization of the latter have been given earlier consideration [7] and will not be considered in detail. Although the materials considered here are essentially cationic and anionic polyelectrolytes (figure 1) [31–35], a common phenomenon is the formation of bundles of multiple strands and diverse shapes in solution phase which stands against chemical intuition. Since association of the strands has been observed in aqueous and organic media, intra- and interstrand repulsive electrostatic interactions are compensated by other interactions that stabilize the bundles such as H-bonds and π–π interactions. Theoretical calculations have shown that hydrogen bonds and π–π interactions stabilize the multistrand bundles of the annulene containing poly([Ni^{II}(tmdbztaa)])polymer [32]. The diverse interactions that stabilize the different shapes observed in TEM and AFM micrographs have been examined in various protonation states of the carboxylate groups. Different protonation states in a single strand lead to the following observations. Deprotonation of all carboxylates in the model generates a linear structure that is retained during the dynamics by internal repulsion of the negative groups. A similar effect results from modeling of a half-protonated single strand, as adjacent carboxylate groups can form intramolecular H-bonds that prevent bending. However, this may be an artifact of the "single-strand" modeling. Full protonation of the carboxylates generates a structure that bends at the ends or winds into a ball showing intramolecular H-bonds from the carboxylate protons to the annulene nitrogens. The "Texas saddle" structure (figure 2) [36] characteristic of the latter in its neutral form is distorted by protonation.

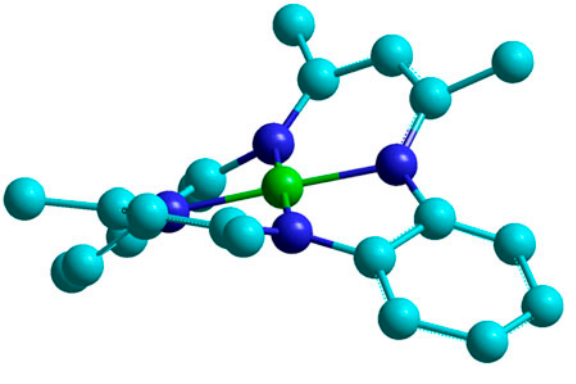

Figure 2. Saddle-shaped structure of [Ni^{II}[tmdbztaa]. Hydrogens are omitted for clarity. The four N atoms (blue) and the Ni (green) are in the same plane, while the phenylene groups are in planes pointing downward the 1,3-dimethylpropylene groups point upward (see http://dx.doi.org/10.1080/00958972.2014.975221 for color version).

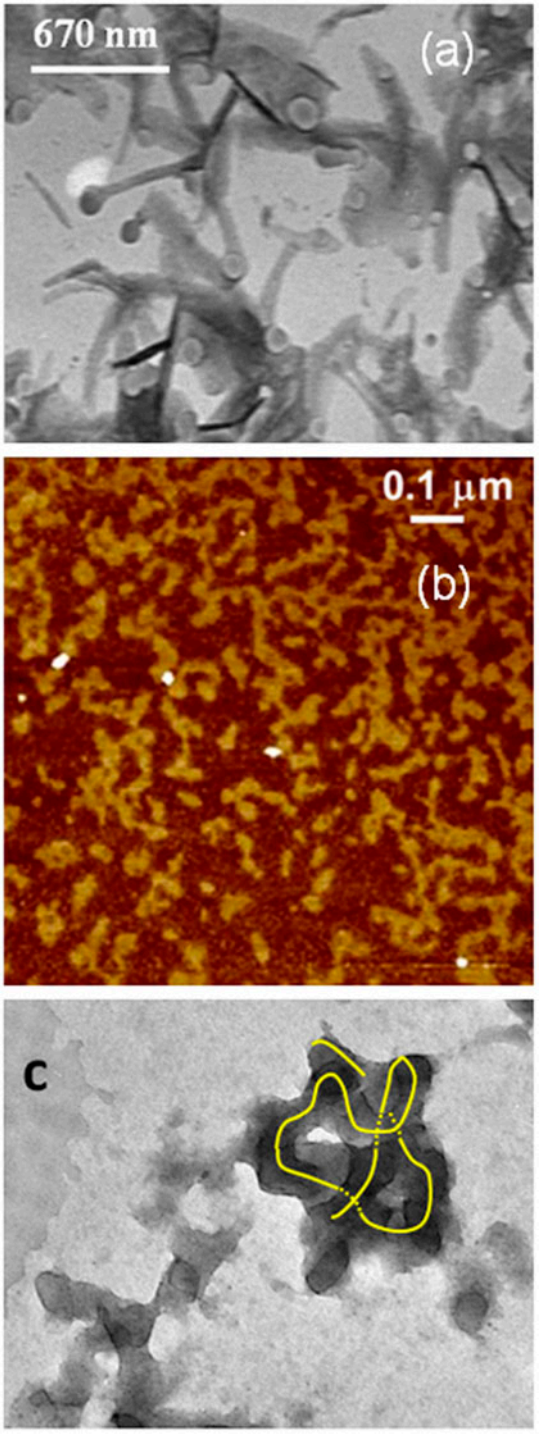

Figure 3. TEM microgrph (a) recorded with poly([Ni^{II}(tmdbztaa)])$_2$ solutions containing 0.1 and 0.01 M $HClO_4$ in CH_3CN. AFM micrograph of the polymer (b) with a sample prepared from an acidic solution of the polymer in CH_3CN. Z scale: 5 nm. TEM structures from basic solutions, (c) A yellow line has been inserted to highlight the shape of the bundle. Scales are indicated in the figure (see http://dx.doi.org/10.1080/00958972.2014.975221 for color version).

When more than one strand is present, the main interactions that glue them together are the interstrand H-bonds between the carboxylate groups, as shown in the figure, although interstrand H-bonds between protons of carboxylic groups and the annulene N atoms are also observed. Because the stabilizing interactions are intrinsic to the pendent coordination complex, so is the stability of the bundles. This is exemplified by the series of polymers poly (Mtspc) containing pendent phthalocyanines of the M = Al(III), Co(II), Ni(II), and Cu(II) ions [31, 33, 34], figure 1(a). While bundles of poly(Altspc) strands are stable over a long period of time, the aggregates of poly(Cutspc) strands dissociate into smaller forms and Cu (II) pendants are simultaneously detached from the polymer backbone over a 24 h period. The poly([Ni^{II}(tmdbztaa)]), figure 1(b), bundles are also medium dependent in both morphology and stability. Bundles with a spherical shape are observed in acidic CH_3CN while stick-like shapes are observed in acidic or basic aqueous solutions (figure 3). Conversion between the morphological shapes, from spherical to stick-like shapes, is caused by a change of the solvent composition. The conversion is slow (~24 h) with pH-dependent kinetics.

There are also examples where the morphology of the polymer (where complexes are to be grafted) remains in the final polymer containing the grafted complexes. The average structure of Rh^{III}(pc) grafted into poly(acrylate) is shown in figure 1(c) [33]. Strands of poly(Rh^{III}(pc)) are shown as strings of spherules under the AF microscope operated in the tapping mode. These spherules were observed with samples of the polymer prepared under different conditions (figure 3), and they are the result of the poly(acrylate) backbone hypercoiling. In a manner, they resemble spherules in the hypercoiled poly(metaacrylate)

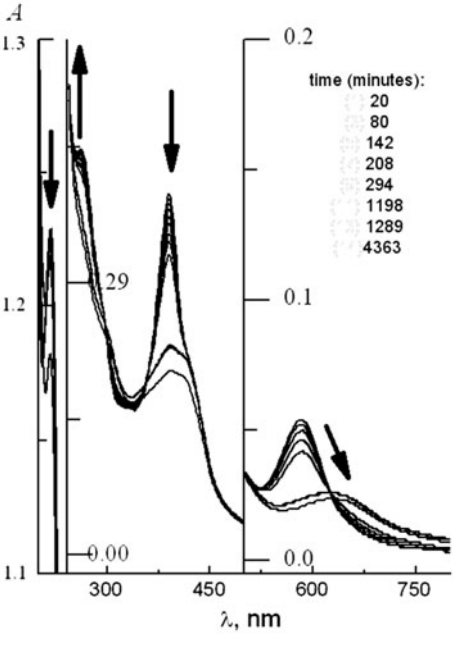

Figure 4. Changes of the poly([Ni^{II}(tmdbztaa)])$_2$ UV–vis absorption spectrum with time due to the annulene ligand protonation. The inset shows delays (in minutes) used when each spectrum was recorded and the arrows show the sense of the change in the spectrum.

[37, 38]. Formation of pendent Rh^{III}(pc)oligomers, principally dimers, contributes to stabilize the hypercoiled spherules which remain unchanged even in acidic media.

Morphological control of the pendent complex reactions

A common characteristic of the morphologies described in the previous section is that in both the strand and the bundles of strands, pendent complexes reside in different environments and are exposed differently to the medium. This condition affects the rates of reactions of the pendent complexes with reactants in the bulk of the solution. Additionally, a slow change in the polymer morphology can be the rate-determining step in the reactions of the pendent complexes with reactants in the bulk of the solution. This mechanism is observed when the pH of a poly([Ni^{II}(tmdbztaa)]) solution is rapidly changed from basic (pH 8 or 10) to acidic (pH 4 or 5) [32], figure 4. Spectroscopic changes in figure 4 correspond to the protonation of the annulene ligand over a period longer than 24 h. In contrast, the protonation of the polymer-free [Ni^{II}(tmdbztaa)] complex takes place within the change of pH. The effect of the morphological change and the exposure of the pendent complexes to different environments are also reflected in the chemical reaction described in the following sections.

Behavior of pendent complexes in thermal redox reactions

Cyclic voltammetry and UV–vis spectra showed that protonation of the annulene ligand of [Ni^{II}(tmdbztaa)] pendent complexes proceeds over periods of 24 h or more. In contrast, the protonation of the polymer-free [Ni^{II}(tmdbztaa)] has a fast rate of a common acid–base neutralization reaction. The pH-dependent rate of the poly([Ni^{II}(tmdbztaa)]) protonation is controlled by slow morphological changes of the polymer bundles from their spherical to stick-like shapes. The morphological change seems to occur through several steps that become evident at pH ≤ 4. The cyclic voltammograms of poly([Ni^{II}(tmdbztaa)]) in aqueous and in DMF/H_2O mixed solvents closely resembled those of the polymer-free [Ni^{II}(tmdbzaa)] [32]. The −1 and −2 electron oxidation of the ligand and the reduction of Ni(II)–Ni(I) occur at nearly the same potentials as in the polymer-free [Ni^{II}(tmdbzaa)]. Furthermore, sequential oxidation–reduction cycles induce redox coupling of neighboring pendent complexes in the same manner observed with polymer-free [Ni^{II}(tmdbztaa)]. Also, the cyclic voltammograms of poly(K_2Co^{II}trspc) and poly(K_3Cu^{II}tspc) show that the phthalocyanine pendants are associated in oligomers (probably dimers) at the low concentrations, where the polymer-free phthalocyaninate complexes, K_4[Cu^{II}tspc] and K_3[Co^{II}trspc], are monomers. Cyclic voltammetry experiments showed no evidence that the phthalocyanine and annulene pendants are in diverse environments in the polymeric matrix. It is possible that the electrode processes only involve those pendent complexes in the bundles that are in the exterior of the bundles of strands. They will be more exposed and in similar environments. In contrast to the electrochemical processes, photochemical reactions of the pendent complexes and their reactions with pulse radiolytically generated radicals reveal the presence of pendent complexes in different environments.

The effect of the strand aggregation in bundles makes the reactions of the pendent Al^{III}(┗NHS(O_2)trspc$)^{2-}$ in poly(HOAl^{III}tspc) more diverse than those of the Al^{III}(tspc$)^{3-}$ [34]. The reactive Al^{III}(┗NHS(O_2)trspc$)^{2-}$ pendent complexes are located in strands of the polymer and the latter associated in bundles. Due to this condition, solutions of the polymer

bear a strong resemblance with solutions of micelles [39, 40]. Because of the aggregation in bundles, large spaces of the solution bulk are devoid of reactive pendent complexes in contrast to the homogeneous distribution of molecules in the $Al^{III}(tspc)^{3-}$ solutions [34]. Consequently, reactions of pulse radiolytically generated radicals ($OH^{\bullet}$, $HCO_3^{\bullet}$, $(CH_3)_2COHCH_2^{\bullet}$, $N_3^{\bullet}$, e_{aq}^-, $CO_2^{\bullet-}$, and $(CH_3)_2C^{\bullet}OH$ have second-order rate constants in excess of those expected for a diffusion-controlled reaction or with values abnormally large for the reactions of a given radical. These abnormally large second-order rate constants are calculated as k_{ob}/[pendants], where k_{ob} is the rate constant calculated under a pseudo-first-order regime and [pendants] is the total concentration of pendent $Al^{III}(\ \llcorner NHS(O_2)trspc)^{2-}$. Rate constants with abnormally large values must be ascribed, therefore, to processes occurring within the pockets in the bundle of strands. In this sense, there is a close resemblance between the reactions of radicals generated within the poly($HOAl^{III}$tspc) aggregates and

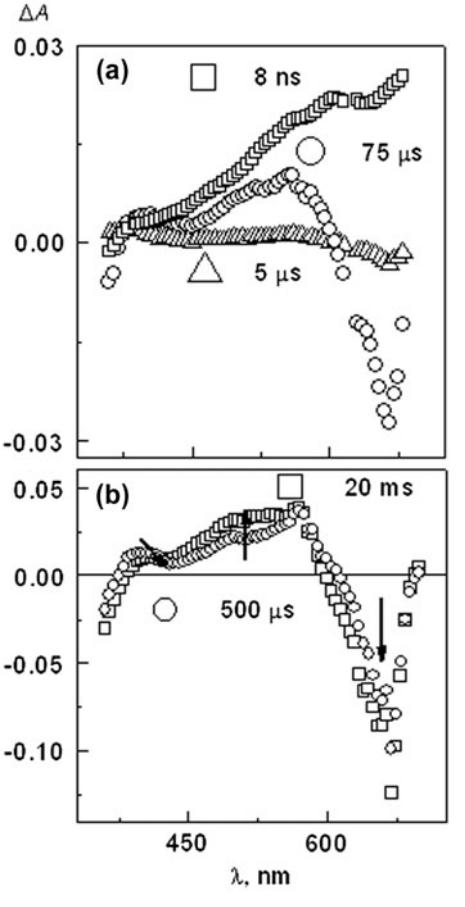

Figure 5. Reaction of poly(Cu^{II}tspc)$^{\backslash 3-}$ with pulse radiolytically generated $CO_2^{\bullet-}$ radicals. Spectral changes in (a) correspond to the parallel formation of the metal-reduced, $Cu^{I}pc(-SO_3)_3(-SO_2N<)^{\backslash 4-}$ and the ligand–radical, $Cu^{II}pc^{\bullet}(-SO_3)_3(-SO_2N<)^{\backslash 4-}$ over a 75 μs period. Changes in the spectrum, shown in (b), correspond to the transformation of $Cu^{I}pc(-SO_3)_3(-SO_2N<)^{\backslash 4-}$ into the ligand–radical $Cu^{II}pc^{\bullet}(-SO_3)_3(-SO_2N<)^{\backslash 4-}$. The conversion of $Cu^{I}pc(-SO_3)_3(-SO_2N<)^{\backslash 4-}$ into $Cu^{II}pc^{\bullet}(-SO_3)_3(-SO_2N<)^{\backslash 4-}$ is responsible of a bleach of the solution at wavelengths of the phthalocyanine Q-band in the 500 μs to 20 ms time domain.

processes occurring with micelle-entrapped substrates [33, 39, 40]. However, a comparison between the rate constants obtained for reactions of various radicals with the pendent complexes show that other factors, such as the mobility of the radical in the aggregate pockets, have also a significant bearing on the reaction rate.

The medium conditions created by the strand and aggregate morphologies lead to the substantial reactivity changes manifested as alterations of the reaction rate and the appearance of new reaction pathways. In experiments using the pulse radiolysis technique, the e^-_{aq}, $C^{\cdot}H_2OH$ or $CO^{\cdot-}_2$ were generated in the presence of poly(K_3Cu^{II}tspc) [35]. The e^-_{aq} and $C^{\cdot}H_2OH$ reduce the phthalocyanine ligand, while $CO^{\cdot-}_2$ produces pendent complexes reduced at both the metal center and the ligand (figure 5). Since the Cu(I) product was only formed when polymer-free $K_4[Cu^{II}tspc]$ was reduced in CH_2Cl_2, a distribution of monomeric and oligomeric pendent complexes exposed to the protic medium of the solution and to the less protic inner space of the bundle account for the formation of the metal and the ligand reduction products. Other factors, such as the coordination of $CO^{\cdot-}_2$ to Cu(II) of the phthalocyanine pendant, must also contribute to the formation of Cu(I) product. Coordination of various radicals $N^{\cdot}_3$, $^{\bullet}OH$, $(CH_3)_2OHCH^{\cdot}_2$ and $CH_2OH^{\bullet}$, to Co(II) pendants of poly(K_2Co^{II}trspc) has been observed. The pendent Co(III)-alkyl product, formed when C-centered radicals are the oxidants, is unstable and decays into a Co(I) product, equations (1) and (2).

$$(CH_3)_2COHC^{\cdot}H_2 + Co^{II}pc(SO_3)_2(SO_2N<)^{\backslash 2-} \rightarrow ((CH_3)_2COHCH_2)Co^{III}pc(SO_3)_2(SO_2N<)^{\backslash 2-} \quad (1)$$

$$((CH_3)_2COHCH_2)Co^{III}pc(SO_3)_2(SO_2N<)^{\backslash 2-} \xrightarrow{OH^-} (CH_3)_2COHCH_2OH + Co^{I}pc(SO_3)_2(SO_2N<)^{\backslash 3-} \quad (2)$$

A reaction with the metal center has been observed also with pendent $Al^{III}(\ ^{\backslash}NHS(O_2)$trspc$)^{2-}$. Pulse radiolytically generated $SO^{\cdot-}_3$ radicals react with either $Al^{III}(tspc)^{3-}$ and pendent $Al^{III}(\ ^{\backslash}NHS(O_2)trspc)^{2-}$ producing similar transient spectra [34]. In both cases, formation of the final product occurs in two steps with strikingly different reaction rates. The difference in reaction rates must be attributed to the polymer effect which makes the $Al^{III}(\ ^{\backslash}NHS(O_2)trspc)^{2-}$ reactions much slower in poly($HOAl^{III}$tspc) than the $Al^{III}(tspc)^{3-}$ one. The first step in the pendent $Al^{III}(\ ^{\backslash}NHS(O_2)trspc)^{2-}$ reaction is attributed to the diffusion and reaction of the radiolytically generated $SO^{\cdot-}_3$ radicals with pendent complexes inside the polymer aggregates. A similar reaction of $Al^{III}(tspc)^{3-}$ in the bulk of the solution has a diffusion-controlled rate. Coordination of $SO^{\cdot-}_3$ radical to Al(III), i.e. replacing OH^- and/or H_2O ligands, is a possible process consistent with the experimental observations (figure 6). Coordination of the $SO^{\cdot-}_3$ radical to either Al(III) centers to form the short-lived intermediate causes little changes in the absorption spectrum, but it will affect the rate of formation of the long-lived intermediate. In the second step of the mechanism, insertion of the $SO^{\cdot-}_3$ radical into the phthalocyanine macrocycle forms a phthalocyanine radical, i.e. the long-lived intermediate. Decay of the $SO^{\cdot-}_3$ adduct to the phthalocyanine macrocycle, i.e. the long-lived intermediate, is faster in $Al^{III}(tspc)^{3-}$, $2k/\varepsilon = 7.3 \times 10^6$ cm s^{-1} than in the pendent $Al^{III}(\ ^{\backslash}NHS(O_2)trspc)^{2-}$, $2k/\varepsilon \approx 2.6 \times 10^3$ cm s^{-1}. An approximately 10^{-4} deceleration of the reaction in the polymer can be attributed to medium conditions inside the aggregates

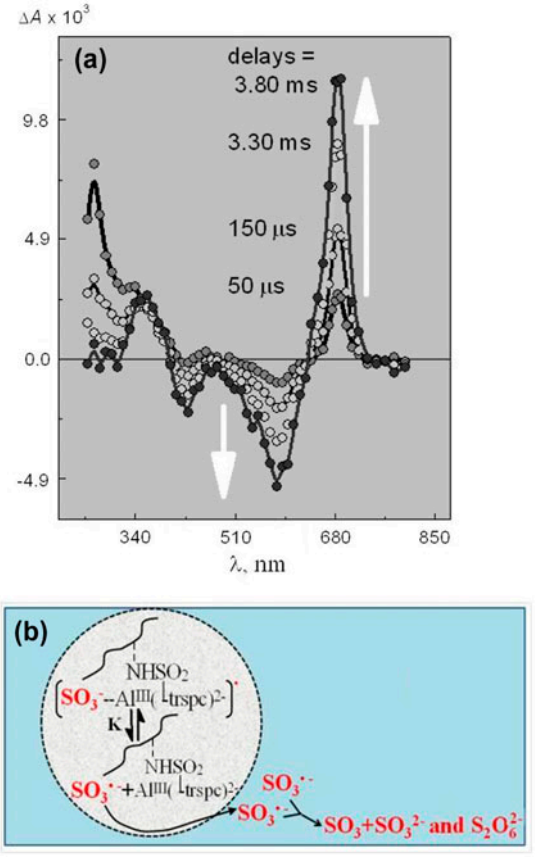

Figure 6. Transient difference spectra (a) are observed when $SO_3^{\bullet-}$ radicals react with $Al^{III}(\llcorner NHS(O_2)trspc)^{2-}$ and a proposed mechanism of the $SO_3^{\bullet-}$ - phthalocyanine adduct decay is shown in (b). A reaction forming an adduct between the $SO_3^{\bullet-}$ radical and $Al^{III}(\llcorner NHS(O_2)trspc)^{2-}$ pendants in a time scale of 4 ms accounts for the transient spectrum in (a). The decay of the adduct takes place in the time domain of 10–70 ms. Spectroscopic changes were recorded with different delays after the radiolytic generation of $SO_3^{\bullet-}$ radicals in a 0.1 M SO_3^{2-} solution buffered at pH 9.5 containing also 1.1×10^{-5} M pendants. Arrows indicate the sense of the change with time. In (b), the aggregate of strands is represented by the circle where K is an equilibrium constant for the dissociation of the adduct in its constituents. $SO_3^{\bullet-}$ radicals that escape from the aggregate undergo disproportionation and/or dimerization with an overall rate constant $2k$. The disappearance of the adduct will be kinetically of a second order with an integrated rate law, $-d[\rho_{adduct}]/dt = (2k\,K/\rho_{pendant}) \times [\rho_{adduct}]^2$, where ρ_{adduct} and $\rho_{pendant}$ are, respectively, the molar densities of adducts and pendants in the aggregate [34].

that provide larger stability to the adduct between $SO_3^{\bullet-}$ radical and the phthalocyanine ligand. Dissociation of the adduct can also be kinetically arrested in pockets of the aggregate. This effect will be similar to reactions of molecular fragments such as a pair of radicals, trapped in the solvent cage or in pockets of a molecular sieve. Both medium conditions and trapping inside the pockets of the aggregates must have a retardation effect on the separation of the $SO_3^{\bullet-}$ radical from the macrocycle. Changes in the absorption spectrum associated with decay of the $SO_3^{\bullet-}$ – phthalocyanine ligand adduct show that pendent $Al^{III}(\llcorner NHS(O_2)trspc)^{2-}$ are regenerated and the rate of the process exhibits an inverse dependence on the concentration of the intermediate [figure 6(a)]. A probable path for the

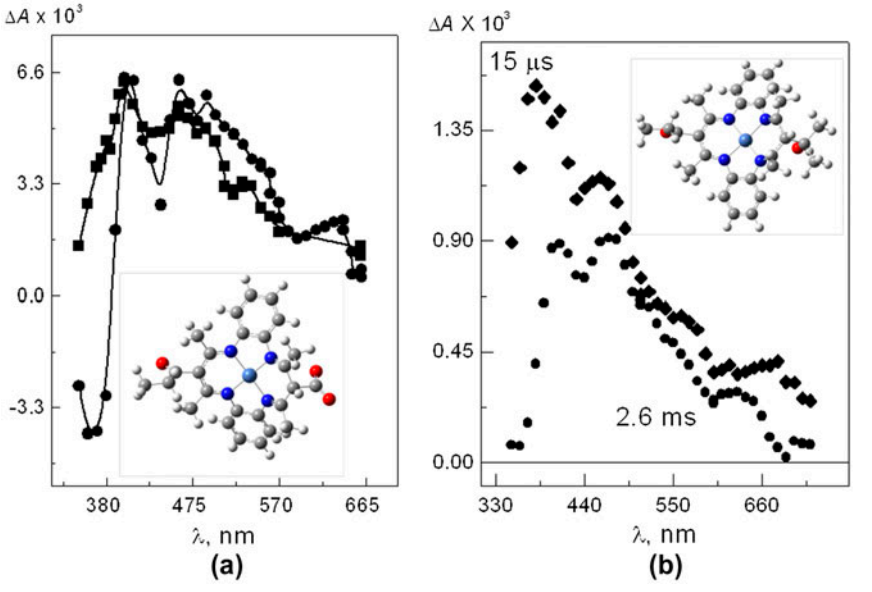

Figure 7. Spectra recorded in pulse radiolysis of N_2O saturated solutions of poly([Ni^{II}(tmdbztaa)])$_2$. In these conditions, the Ni(II) pendants were reduced: (a) by either $CO_2^{\cdot-}$ (○) or $(CH_3)_2C^{\cdot}OH$ (□). In (b) N_2O was replaced by N_2 and e_{aq}^-, and $(CH_3)_2C^{\cdot}OH$ are the generated reactants. Therefore, the pendants are reduced by the combined actions of e_{aq}^- and $(CH_3)_2C^{\cdot}OH$. Spectra recorded with delays as short as 15 μs, figure 7(b) (◇), exhibited bands with λ_{max} = 390 and 460 nm. The intensity and positions of these peaks are considerably different than those (λ_{max} = 405 and 472 nm) observed in the spectra of the species generated by the $(CH_3)_2C^{\cdot}OH$ radicals alone, figure 7(a) (○). They were attributed to a product of the fast reaction of the pendants with e_{aq}^-. The growth of this product spectrum, nearly ~ 40 times faster than the observed reaction between the pendants and $(CH_3)_2C^{\cdot}OH$, sets apart the respective reactions of the $(CH_3)_2C^{\cdot}OH$ radical and e_{aq}^- with [Ni^{II}(tmdbztaa-CO- - -)] pendants. An inset to (a) and (b) are, respectively, the optimized structures of the equations (3) and (4) products. Delays from the radiolytic pulse used recording the spectra are: (○) 500 μs, (□) 300 μs in (a) and (◇) 15 μs, (□) 2.6 ms in (b).

decay involves diffusion of $SO_3^{\cdot-}$ radicals out of the aggregates followed by rapid radical–radical annihilation in the bulk of the solution [figure 6(b)]. Adducts of radicals to the ligand have also been observed when poly([Ni^{II}(tmdbztaa)]) bundles react with C-centered radicals (figure 7) [32]. Minimal differences were observed between spectra of the products, respectively, generated by the $CO_2^{\cdot-}$ and $(CH_3)_2C^{\cdot}OH$ reactions with the pendent complexes. These transient spectra cannot be assigned to [Ni^{I}(tmdbztaa-CO- - -)]$^-$ products because reduction potentials of the $CO_2/CO_2^{\cdot-}$ and $(CH_3)_2CO/(CH_3)_2C^{\cdot}OH$ couples are insufficiently negative to drive the reductions of the metal center or other groups in the backbone. Therefore, the transient spectra were associated with species produced either by coordination of the radicals to the metal center or to addition of radicals to the annulene ligand. Calculations of the absorption spectra of these potential products support the assignments of the transient spectra to chromophores that are adducts of the radicals to the annulene macrocycle, equations (3) and (4).

$$\left[Ni^{II}\left(\text{tmdbzTAA-}\dot{\underset{\vdots}{C}}=O\right)\right] \xrightarrow{CO_2^{\cdot-}} \left[Ni\left(O_2C-\text{tmdbzTAA-}\dot{\underset{\vdots}{C}}=O^{\cdot}\right)\right]^- \qquad (3)$$

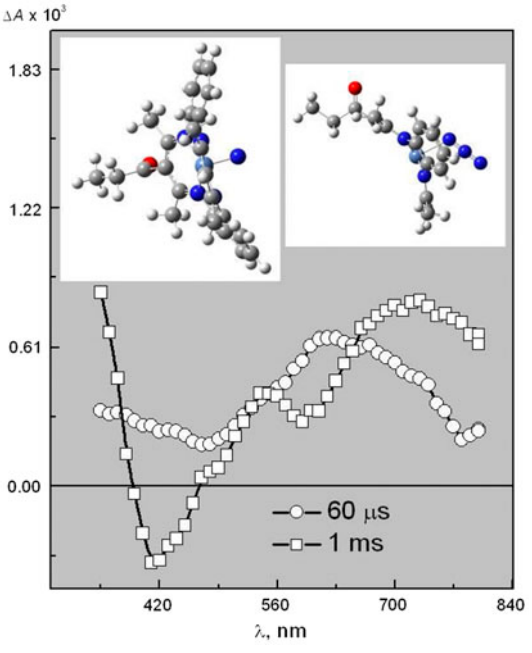

Figure 8. Transient spectra recorded when radiolytically generated $N_3^{\bullet}$ radicals react with poly([Ni^{II}(tmdbztaa)])$_2$. The delays from the $N_3^{\bullet}$ radicals generation are indicated in the figure. The insets show the optimized structures of pendants with an N_3^- coordinated to the Ni (top right) and the nitrene complex (top left). Nitrogens of these two groups are colored blue (see http://dx.doi.org/10.1080/00958972.2014.975221 for color version).

$$\left[Ni^{II}\left(\text{tmdbzTAA-}\overset{\vdots}{C}=O\right)\right] \xrightarrow{(CH_3)_2C^{\bullet}OH} \left[Ni\left((CH_3)_2(HO)C\text{-tmdbz-}\overset{\vdots}{C}=O^{\bullet}\right)\right] \quad (4)$$

Optimized structures obtained from the calculations are shown in the insets to figure 6(a) and (b), respectively, and show that the adducts of the $CO_2^{\bullet-}$ and $(CH_3)_2C^{\bullet}OH$ radicals to the annulene ligand can be regarded as Ni(II)–ligand radical moieties. The addition of the radicals to the ligand stands in contrast with the reaction of $N_3^{\bullet}$ radical with [Ni^{II}(tmdbztaa-CO- - -)] pendants. Coordination of the $N_3^{\bullet}$ radical to the metal center of the pendants occurs in a first step that is followed by rearrangement into a longer lived Ni–nitrene complex, equations (5) and (6) and figure 8.

$$\left[Ni^{II}\left(\text{tmdbzTAA-}\overset{\vdots}{C}=O\right)\right] \xrightarrow{N_3^{\bullet}} \left[Ni\left(O_2C-\text{tmdbzTAA-}\overset{\vdots}{C}=O\right)N_3\right] \quad (5)$$

$$\left[Ni^{II}\left(\text{tmdbzTAA-}\overset{\vdots}{C}=O\right)\right] \rightarrow \left[NNi\left(O_2C-\text{tmdbzTAA-}\overset{\vdots}{C}=O\right)\right] + N_2 \quad (6)$$

The optical spectrum calculated using the theoretically optimized structure of the Ni–nitrene pendant agreed with the pulse radiolytically observed spectrum of the long-lived transient [41].

Photochemical and photophysical processes

The morphological features of the strands and bundles of strands force pendent complexes to be in close proximity (figure 9). Therefore, absorption of light produces excited states of

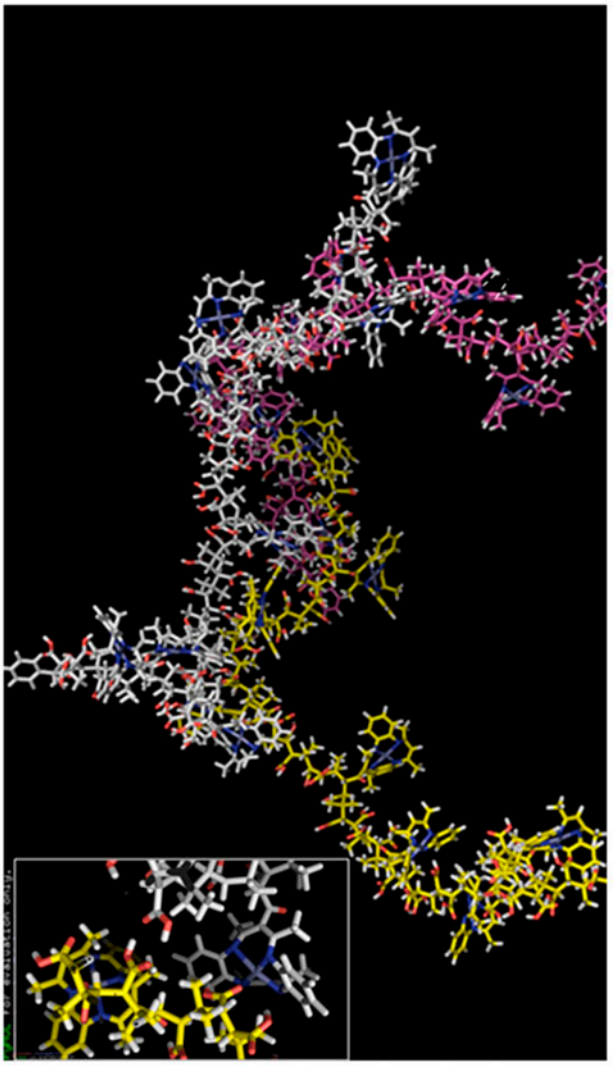

Figure 9. Structure of bundle obtained after a short molecular dynamic simulation of three strands of poly $([Ni^{II}(tmdbztaa)])_2$ with a fully protonated backbone. It shows those interactions holding the strands together including H-bonds between the OH groups of the backbone and the annulene pendant. The inset is an expanded view of the H-bond interaction between carboxylate groups in different strands helping to stabilize the aggregation.

the pendent complexes which are in close proximity to pendent complexes in the ground state and/or to other electronically excited pendent complexes. If solutions of the polymer-free complexes were used instead of the polymer-grafted ones, the creation of similar conditions requires orders of magnitude larger concentrations of the complexes and/or light intensities. In addition to producing the simultaneous creation of two neighboring electronically excited pendent complexes by absorption of light, the experimental evidence has shown that migration of energy is possible, for example via a Forster energy transfer mechanism from one electronically excited pendent complex to another in the ground state [31, 32, 42, 43]. This energy hopping through the bundle has been observed in the photochemical processes of a number of polymers with grafted coordination complexes such as poly(HOAl^{III}tspc) [31]. Since the strands of poly(HOAl^{III}tspc) are associated in near spherical bundles with ~150 nm diameter in aqueous solutions, there is a very large concentration of pendent Al^{III}($\llcorner$NHS(O$_2$)trspc)$^{3-}$ (= pendant^{3-}) inside the bundle. Most of these pendent complexes in the bundles form π-stacks where the largest fraction of them must be dimers, {pendant^{3-} pendant^{3-}}. Flash photochemical observations in a 0.15 ps to 100 μs time domain reveal the photogeneration of electronically excited pendent complexes and the subsequent formation of pendent radicals, pendant$^{\bullet\ 2-}$, and pendant$^{\bullet\ 4-}$. This process stands in contrast with the photochemistry that Al^{III}(tspc)$^{3-}$ shows under the same experimental conditions of poly(HOAl^{III}tspc). Indeed, the kinetics of the phthalocyanine radicals formation and disappearance in poly(HOAl^{III}tspc) is consistent with energy and charge transfer between phthalocyanine pendants in the bundle, equations (7–10).

$$\text{pendant}^{3-} \xrightarrow{h\nu} {}^{S\,or\,T}\text{pendant}^{3-} \tag{7}$$

$$\{\text{pendant}^{3-}\ \text{pendant}^{3-}\} \xrightarrow{h\nu} \{{}^{S\,or\,T}\text{pendant}^{3-}\ \text{pendant}^{3-}\} \tag{8}$$

$$2\ \{{}^{T}\text{pendant}^{3-}\ \text{pendant}^{3-}\} \rightarrow\ \text{pendant}^{\bullet 4-} + \text{pendant}^{\bullet 2-} + 2\ \text{pendant}^{3-} \tag{9}$$

$$\text{pendant}^{\bullet 4-} + \text{pendant}^{\bullet 2-} \rightarrow 2\ \text{pendant}^{3-} \tag{10}$$

A closely related phenomenon was observed in the photochemistry of poly([Ni^{II}(tmdbztaa)]). Irradiations of the polymer at 532 or 351 nm produce charge-separated macrocyclic pendants, CS, with a lifetime $\tau \sim 30$ ns. CS reacts with electron donors and acceptors before it decays with a lifetime $\tau \sim 1$ μs. In parallel to the decay of CS, an excited state–excited state annihilation process gives rise to luminescence whose spectrum spans wavelengths shorter than the wavelength of the irradiation, $\lambda_{ex} > 500$ nm. The spectroscopic features of the luminescence are a broad and structured spectrum that spans significantly over wavelengths shorter than the exciting wavelengths, $\lambda_{ex} = 532$ and 580 nm. The structured emission band is characteristic of an emitting excited state with considerable annulene ligand-centered character, and in order to explain the emission of light at wavelengths much shorter than the wavelengths of the absorbed light, an energy accretion mechanism must be invoked. The experimental observation can be rationalized by a mechanism that involves

the excited state–excited state annihilation to produce an emissive $(HOMO\text{-}6)^1(LUMO)^1_{\text{-dd}'}$ excited state, equations (11) and (12).

$$\left[Ni^{II}\left(tmdbzTAA\text{-}\overset{\vdots}{C}{=}O\right)\right] \overset{+h\nu}{\rightarrow} (HOMO\text{-}1)^1(LUMO)^1_{-dd'}\left[Ni^{II}\left(tmdbzTAA\text{-}\overset{\vdots}{C}{=}O\right)\right] \tag{11}$$

$$\begin{aligned} &2(HOMO\text{-}1)^1(LUMO)^1_{-dd'}\left[Ni^{II}\left(tmdbzTAA\text{-}\overset{\vdots}{C}{=}O\right)\right] \\ &\rightarrow \left[Ni^{II}\left(tmdbzTAA\text{-}\overset{\vdots}{C}{=}O\right)\right] \\ &\quad + (HOMO\text{-}6)^1(LUMO)^1_{-dd'}\left[Ni^{II}\left(tmdbzTAA\text{-}\overset{\vdots}{C}{=}O\right)\right] \end{aligned} \tag{12}$$

There are also photophysical differences between the polymer-free and polymer-grafted complexes due to the presence of the latter in the environment of the polymer bundles. In aqueous solutions of poly-Rh^{III}(pc), stacks of pendent $-CO_2Rh^{III}$(pc) in hydrophobic pockets of the strand account for differences among the photophysical processes of the pendent complexes and those of XRh^{III}(pc), X = Cl, Br, I. These differences are shown in figure 10. The most marked difference is the photogeneration of an excited state with the spectrum and lifetime of a ligand field, LF, excited state not observed when XRh^{III}(pc) complexes were irradiated in homogeneous solution. In addition, the efficiency of the lowest phthalocyanine-centered excited state, $(^3\pi\pi^*)_1$, to undergo electron transfer reactions is decreased in relation to similar reactions of the $(^3\pi\pi^*)_1$ in XRh^{III}(pc). Such a decrease in the efficiency of the $(^3\pi\pi^*)_1$ to undergo electron transfer reactions can be related to the $(^3\pi\pi^*)_1$ to ^{3}LF conversion in poly-Rh^{III}(pc), a process that was not previously observed in the photophysics of XRh^{III}(pc).

Applications to photocatalysis

It is shown in previous sections how the polymer's morphology affects the thermal and photochemical reactions of the pendent complexes. Various practical applications resulting from the morphologically-modified reactivities of the grafted complexes can be envisioned. Two examples that have recently been investigated will be presented next. For many decades, numerous chemical processes for the degradation of lignin, many using transition metal compounds, have been investigated and the subject is still a matter of major efforts. Different motivations explain the great attention that these processes receive [44–51]. The decomposition of lignin (figure 10) was observed in the steady-state photolysis ($\lambda_{ex} \geq 500$ nm) of an aerated solution of lignin that also contained poly($HOAl^{III}$tspc) [30]. An exhaustive photolysis of ~5 h revealed that although the lignin decomposition was close to complete (~95% decomposed), there was no appreciable degradation of the poly($HOAl^{III}$tspc). Based on the experimental evidence, both the photogenerated $O_2^{\bullet -}$ and pendant$^{\bullet 2-}$ radicals must participate in the lignin oxidative degradation. Given the different mobilities

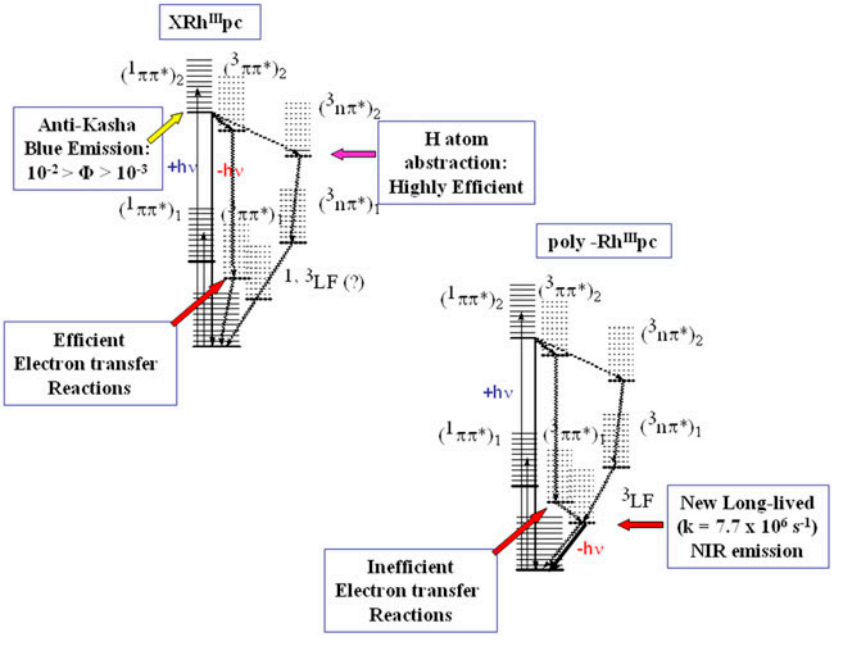

Figure 10. Comparison of the Jablonsky energy diagrams for monomeric $XRh^{III}(pc)$, top left, and $-CO_2Rh^{III}(pc)$ pendants in poly-$Rh^{III}(pc)$, bottom right. The question mark in the top diagram shows where LF excited states of Rh(III) could be expected to be in the $XRh^{III}(pc)$ monomer. The most marked difference is the photogeneration of an excited state with the spectrum and lifetime of a ligand field, LF, excited state not observed when $XRh^{III}(pc)$ complexes were irradiated in homogeneous solution. In addition, the efficiency of the lowest phthalocyanine-centered excited state, $(^3\pi\pi^*)_1$, to undergo electron transfer reactions is decreased in relation to similar reactions of the $(^3\pi\pi^*)_1$ in $XRh^{III}(pc)$. The decrease in the efficiency $(^3\pi\pi^*)_1$ to undergo electron transfer reactions can be related to the $(^3\pi\pi^*)_1$ to ^3LF conversion in poly-$Rh^{III}(pc)$, a process that was not previously observed in the photophysics of $XRh^{III}(pc)$.

of these radicals, the most probable steps in the mechanism are oxidation of the lignin by $O_2^{\bullet-}$ followed by a slow reaction of the pendant$^{\bullet 2-}$ with radicals generated from the lignin oxidation. The latter process must be able to close the photocatalytic cycle of the poly ($HOAl^{III}tspc$).

In a practical application of poly($[Ni^{II}(tmdbztaa)]$), the migration of energy and charge through the Ni(II) pendant-crowded arrangements in a strand or bundle of strands becomes accessible under much more gentle conditions than those required in solutions of the polymer-free $[Ni^{II}(tmdbztaa)]$ complex [32]. This chemistry is therefore better suited to photocatalysis in aqueous homogeneous solution. The applicability of these systems to the reduction of CO_2 to CO should be highlighted as the most striking result of the poly ($[Ni^{II}(tmdbztaa)]$) chemistry. In the endothermic reduction of CO_2 to CO by HSO_3^-/SO_3^{2-} where the grafted nickel(II) complex has the dual role of an antenna and a catalyst is used as a test of the complex catalytic capability. The reaction, equation (13), as written is thermodynamically disfavored by +186.36 kJ/mol.

$$SO_2(g) + CO_2(g) \rightarrow SO_3(g) + CO(g) \quad \Delta G^0 = 186.36 \text{ kJ/mol} \tag{13}$$

This energy deficit corresponds to a wavelength for photoactivation of 642 nm. In aqueous solution at pH 8, the appropriate reaction is also disfavored but with a smaller energy deficit, equation (14).

$$SO_2 \cdot xH_2O + CO_2(aq) \rightarrow SO_4^{2-} + CO + 2H^+ \quad \Delta G^0 \geq 70 \text{ kJ/mol} \tag{14}$$

Consequently, this reaction can be photoactivated with visible light with a catalytic reagent that incorporates an absorption antenna. Under these conditions, poly([Ni^{II}(tmdbztaa)])$_n$ becomes a catalyst of practical importance, useful for storage of energy.

Conclusion

The grafting of the phthalocyanine and tmdbztaa metallo complexes into a polymer backbone allows dissolution in solvents where they are intrinsically insoluble. Dissolving them in these solvents results in modifications of the complexes chemical reactivity (particularly in medium-dependent photochemical reactions). Solvent induced morphological modifications of the polymer strands and aggregates of strands add a new element of control over the complexes reaction pathways. In consequence, reaction products formed only in an organic solvent are obtained in aqueous solutions of the polymers. Also, these reactivity changes can be related to the pendent complexes being placed in close proximity within pockets in the strands and strand aggregates. The proximity between the grafted complexes is a unique characteristic not attained in solutions of the polymer-free phthalocyanine and tmdbztaa metallo complexes. These features of these polymers have been evidenced using only a limited number of complexes with a narrow set of chemical reactions. Much more can be learned when both are expanded. In terms of the control of the chemical reactions, it will be of interest to compare the chemical reactivity of complexes grafted into polymer backbones having groups $–CO_2R$ (where R can be a polycyclic aromatic group) instead of $–CO_2H$. Whether they facilitate or impede the migration of charge and/or energy through the stands and aggregate of strands may provide an additional element of control upon the reactions of the grafted complexes.

Abbreviations

tmdbztaa	5,7,12,14-tetramethyldibenzo[b,i]-1,4,8,11-tetraaza[14]annulene
tspc	phthalocyaninetetrasulfonate
trspc	phthalocyaninetrisulfonate
pc	phthalocyanine
TEM	transmission electron microscope
AFM	atomic force microscope
e^-_{aq}	solvated electron in aqueous solutions
e^-_{sol}	solvated electron in organic medium
k_{ob}	experimentally determined pseudo-first order rate constant
k/ε	ratio of the second order rate constant to the extinction coefficient at the wavelength of the probe
λ_{ex}	wavelength of the light used for the irradiation of the light absorbing compound $(HOMO\text{-}6)^1(LUMO)^1_{\text{-dd}}$
$^3\pi\pi^*$	triplet excited state resulting in an electronic transition between low energy π and higher energy π^* orbitals
^{3}LF	triplet metal-centered excited state

Abbreviated names of the polymers with their corresponding structures can be seen in figure 1.

References

[1] A. Gasnier, C. Bucher, J.-C. Moutet, G. Royal, E.S.-A. Pierre Terech. *Macromol. Symp.*, **304**, 87 (2011).
[2] S.-J. Liu, Y. Chen, W.-J. Xu, Q. Zhao, W. Huang. *Macromol. Rapid Commun.*, **33**, 461 (2012).
[3] W.Y. Tam, C.S.K. Mak, A.M.C. Ng, A.B. Djurišić, W.K. Chan. *Macromol. Rapid Commun.*, **30**, 622 (2009).
[4] C.A. Fustin, P. Guillet, U.S. Schubert, J.F. Gohy. *Adv. Mater.*, **19**, 1665 (2007).
[5] S.J. Buwalda, P.J. Dijkstra, J. Feijen. *J. Polym. Sci. A: Polym. Chem.*, **50**, 1783 (2012).
[6] A.L. Lewis, J.D. Miller. *Polymer*, **34**, 2453 (1993).
[7] M. Kaneko, E. Tsuchida. *J. Polym. Sci. Macromol. Rev.*, **16**, 397 (1981).
[8] B. Happ, C. Friebe, A. Winter, M.D. Hager, U.S. Schubert. *Eur. Polym. J.*, **45**, 3433 (2009).
[9] S. Schmatloch, A.M.J. van den Berg, A.S. Alexeev, H. Hofmeier, U.S. Schubert. *Macromolecules*, **36**, 9943 (2003).
[10] M.P. Donzello, C. Ercolani, K.M. Kadish, G. Ricciardi, A. Rosa, P.A. Stuzhin. *Inorg. Chem.*, **46**, 4145 (2007).
[11] Q. Zeng, M. Li, D. Wu, C. Liu, S. Lei, S. An, C. Wang. *Cryst. Growth Des.*, **7**, 1497 (2007).
[12] N. McCann, G.A. Lawrance, Y.-M. Neuhold, M. Maeder. *Inorg. Chem.*, **46**, 4002 (2007).
[13] F. Cuenot, M. Meyer, E. Espinosa, R. Guilard. *Inorg. Chem.*, **44**, 7895 (2005).
[14] M. Meyer, L. Frémond, E. Espinosa, R. Guilard, Z. Ou, K.M. Kadish. *Inorg. Chem.*, **43**, 5572 (2004).
[15] M.-S. Liao, J.D. Watts, M.-J. Huang. *J. Phys. Chem. A*, **109**, 7988 (2005).
[16] A.N. Vedernikov, M. Pink, K.G. Caulton. *Inorg. Chem.*, **43**, 4300 (2004).
[17] D.B. Rorabacher. *Chem. Rev.*, **104**, 651 (2004).
[18] L.M. Mirica, X. Ottenwaelder, T.D.P. Stack. *Chem. Rev.*, **104**, 1013 (2004).
[19] E.A. Lewis, W.B. Tolman. *Chem. Rev.*, **104**, 1047 (2004).
[20] G. Chaka, J.L. Sonnenberg, H.B. Schlegel, M.J. Heeg, G. Jaeger, T.J. Nelson, L.A. Ochrymowycz, D.B. Rorabacher. *J. Am. Chem. Soc.*, **129**, 5217 (2007).
[21] J.W. Sibert, P.B. Forshee, G.R. Hundt, A.L. Sargent, S.G. Bott, V. Lynch. *Inorg. Chem.*, **46**, 10913 (2007).
[22] C.P. Kulatilleke. *Polyhedron*, **26**, 1166 (2007).
[23] G. Gasser, M.J. Belousoff, A.M. Bond, Z. Kosowski, L. Spiccia. *Inorg. Chem.*, **46**, 1665 (2007).
[24] W.L. Man, W.W.Y. Lam, W.Y. Wong, T.C. Lau. *J. Am. Chem. Soc.*, **128**, 14669 (2006).
[25] G. McRobbie, G.C. Valks, C.J. Empson, A. Khan, J.D. Silversides, C. Pannecouque, E. De Clercq, S.G. Fiddy, A.J. Bridgeman, N.A. Young, S.J. Archibald. *J. Chem. Soc., Dalton Trans.*, 5008 (2007).
[26] M.M. Rosenkilde, L.O. Gerlach, S. Hatse, R.T. Skerlj, D. Schols, G.J. Bridger, T.W. Schwartz. *J. Biol. Chem.*, **282**, 27354 (2007).
[27] T. Hunter, I.J. McNae, X. Liang, J. Bella, S. Parsons, M.D. Walkinshaw. *Proc. Natl. Acad. Sci. USA*, **102**, 2288 (2005).
[28] R.H. Holm, P. Kennepohl, E.I. Solomon. *Chem. Rev.*, **96**, 2239 (1996).
[29] P. Antunes, R. Delgado, M.G.B. Drew, V. Félix, H. Maecke. *Inorg. Chem.*, **46**, 3144 (2007).
[30] G.T. Ruiz, M.P. Juliarena, G. Ferraudi, A.G. Lappin, W. Boggess, M.R. Feliz. *Polyhedron*, **38**, 36 (2012).
[31] G.T. Ruiz, G. Ferraudi, A.G. Lappin. *J. Photochem. Photobiol. A: Chem.*, **206**, 1 (2009).
[32] G.T. Ruiz, G. Estiu, J. Costamagna, M. Villagran, C. Vericat, A.G. Lappin, G. Ferraudi. *RSC Adv.*, **4**, 53157 (2014).
[33] S. Thomas, G. Ruiz, G. Ferraudi. *Macromolecules*, **39**, 6615 (2006).
[34] G.T. Ruiz, A.G. Lappin, G. Ferraudi. *J. Polym. Sci. A: Polym. Chem.*, **50**, 2507 (2012).
[35] G.T. Ruiz, A.G. Lappin, G. Ferraudi. *J. Porphyrins Phthalocyanines*, **14**, 69 (2010).
[36] (a) F.A. Cotton, J. Czuchajowska. *Polyhedron*, **9**, 2553 (1990); (b) P. Mountford. *Chem. Soc. Rev.*, **27**, 105 (1998).
[37] K.P. Gniggino, K.L. Tan. In *Polymer Photophysics*, D. Phillips (Ed.), Chap. 7, pp. 341–375, Chapman and Hall, New York, 1985; and references therein.
[38] S.M. Hubig, M.A.J. Rodgers. *J. Phys. Chem.*, **94**, 1933 (1990).
[39] A. Roodt, J.C. Sullivan, D. Meisel, E. Deutsch. *Inorg. Chem.*, **30**, 4545 (1991).
[40] A.J.W.G. Visser, J.H. Fendler. *J. Phys. Chem.*, **86**, 947 (1982).
[41] G. Ferraudi, A.G. Lapin, G. Estiu. unpublished observations.
[42] L.L.B. Bracco, M.P. Juliarena, G.T. Ruiz, M.R. Féliz, G.J. Ferraudi, E. Wolcan. *J. Phys. Chem. B*, **112**, 11506 (2008).
[43] E. Wolcan, G.J. Ferraudi. *Phys. Chem. A*, **104**, 9281 (2000).
[44] B. George, E. Suttie, A. Merlin, X. Deglise. *Polym. Degrad. Stab.*, **88**, 268 (2005).
[45] K.K. Pandey, T. Vuorinen. *Polym. Degrad. Stab.*, **93**, 2138 (2008).

[46] J.J. Bozell, B.R. Hames. *J. Org. Chem.*, **60**, 2398 (1995).
[47] V. Arantes, A.M. Ferreira Milagres. *J. Hazard. Mater.*, **141**, 273 (2007).
[48] K. Ruuttunen, V. Tarvo, J. Aittamaa, T. Vuorinen. *Nord. Pulp Pap. Res. J.*, **21**, 303 (2006).
[49] A.E.H. Machado, J.A. de Miranda, R.F. de Freitas, E.T.F.M. Duarte, L.F. Ferreira, Y.D.T. Albuquerque, R. Ruggiero, C. Sattler, L. de Oliveira. *J. Photochem. Photobiol. A: Chem.*, **155**, 231 (2003).
[50] J. Dec, K. Haider, J.-M. Bollag. *Chemosphere*, **52**, 549 (2003).
[51] J. Blanco, S. Malato, P. Fernández, A. Vidal, A. Morales, P. Trincado, J.C. Oliveira, C. Minero, M. Musci, C. Casalle, M. Brunotte, S. Tratzky, N. Dischinger, K.-H. Funken, C. Sattler, M. Vincent, M. Collares-Pereira, J.F. Mendes, C.M. Rangel. *Solar Energy*, **67**, 317 (1999).